

Segmentation and length measurement of the abdominal blood vessels in 3-D MRI images

Danilo Babin, Ewout Vansteenkiste, Aleksandra Pižurica and Wilfried Philips

Abstract—In diagnosing diseases and planning surgeries the structure and length of blood vessels is of great importance. In this research we develop a novel method for the segmentation of 2-D and 3-D images with an application to blood vessel length measurements in 3-D abdominal MRI images. Our approach is robust to noise and does not require contrast-enhanced images for segmentation. We use an effective algorithm for skeletonization, graph construction and shortest path estimation to measure the length of blood vessels of interest.

I. INTRODUCTION

Certain diseases have an influence on the length of the aortic blood vessels of the abdomen. In diagnosing such diseases a method to compare the lengths of blood vessels of interest to the length of healthy blood vessels can be of great importance. Our goal is to segment the abdominal aorta from the set of 3-D MRI images and apply binary skeletonization algorithm in order to calculate the length of the blood vessels of interest.

There exist a significant number of methods based on mathematical morphology [1], commonly used for medical image segmentation. Two fundamental morphological operators used are erosion and dilation. For these operators the structuring element is an object of carefully chosen shape and size to best correspond to the shape of the object intended for segmentation. Based on these operators, opening and closing operators are defined as sequential dilation after erosion and erosion after dilation, respectively. This way priorities are assigned to either darker or brighter objects in the image. A more advanced approach is explained in [2], where morphological profiles and differential morphological profiles are used that represent a composition of morphological openings and closings with increasing size of the structuring element. This method is prone to errors in the size of segmented regions and is not robust to noise. An improvement to this is proposed in [3], where the solution is to examine the differences between the original pixel value and the value of the opening or the closing at the given scale, depending on which of these has the highest value. However, this method assigns a value to a pixel based on the pixel values of the structuring element, which introduces a problem of a proper threshold value selection in order for all the blood vessels to get segmented. The threshold value would have to vary

not only between neighboring slices, but also for different object in the same slice, making this method inapplicable in our case.

Instead of assigning a background value or a foreground value to the processed pixel for the certain structuring element, we propose a method that compares the pixel value to the average value of all pixels in the structuring element. The value we assign to the processed pixel is equal to the maximum size of the structuring element, thus prioritizing to similar structures, and making the segmentation process less dependent on individual pixel values. Most of the related works on this topic use angiography images (which are obtained by a half-invasive method of injection of contrast substance into the blood vessels) [4], and the developed algorithms are not applicable on data sets which are not contrast-enhanced. The main advantage of our method is that we designed it for an application on images that are not contrast-enhanced, but which can be successfully applied to contrast-enhanced images as well. The proposed method takes into account the value and the morphology of the object to be segmented, while being robust to noise and sudden changes in shape in the case of the 3-D data sets. Our method stands out in situations when contrast-enhanced images can not be obtained or if the segmentation and length measurement results need to be obtained in a short period of time.

II. THE PROPOSED METHOD

In order to make our method robust to noise and sudden changes in intensity of objects in neighboring slices, we base our method on a combination of structure, size and average intensities of the object for segmentation. Our approach is to measure the extent to which equidistant pixels “influence” the currently processed pixel. We do this by comparing the ratio of the average value of the equidistant neighborhood and the value of the processed pixel to the predefined segmentation coefficient. This method shows robustness to noise because the result of the segmentation depends on the wider neighborhood of the pixel, thus relying more on the structure of the neighboring pixels than on their values which are corrupted by noise. The new value of the pixel is equal to the number of sequential radii for which the calculated ratio does not exceed the predefined segmentation coefficient. We segment the image either by comparison to the maximum distance inside the image or by setting a threshold function corresponding to the maximum radius of the object that we want to segment.

All authors are with Department of Telecommunications and Information Processing-TELIN-IPi-IBBT, Faculty of Sciences, Ghent University, Sint-Pietersnieuwstraat 41, B-9000 Ghent, Belgium.

Danilo Babin: dbabin@telin.ugent.be

Ewout Vansteenkiste: ervsteen@telin.ugent.be

Aleksandra Pižurica: sanja@telin.ugent.be

Wilfried Philips: philips@telin.ugent.be

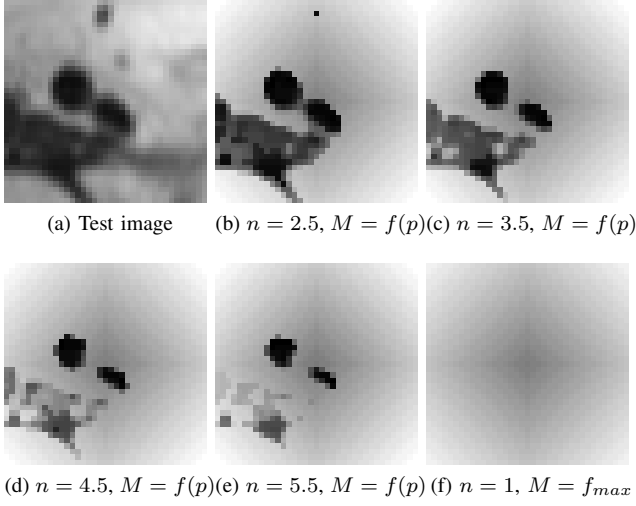


Fig. 1: Original test image (37×37) in (a), transformed images for different values of parameter n in (b), (c), (d), (e), and the image of maximum pixel distances (f).

Let $p \in \mathbb{Z}^2$ denote the pixel of image I in the discrete Cartesian grid with a value $f(p)$ from a range of continuous gray scale values $f(p) \in [f_{min}, f_{max}]$. For a given point p of the image I , with coordinates (x_p, y_p) we define the set of equidistant pixels at the radius $r \in \mathbb{N}$ as in (1).

$$E_r(p) : \{q \in I \mid (r-1)^2 < (q-p)^2 \leq r^2\} \quad (1)$$

For this set the sum of all values can be expressed as in (2):

$$S_r(p) = \sum_x \sum_y f(x, y), \quad (x, y) \in E_r(p), \quad r \in \mathbb{N} \quad (2)$$

In (3) we assign a new value for the pixel p equal to the maximum radius value R , such that for all radius values $r \in \{1, \dots, R\}$ the average value of all equidistant pixels does not exceed the predefined segmentation coefficient n :

$$d_n(p) = \max_R \left(\forall r \in \{1, \dots, R\}, \left| \frac{S_r(p)}{N_r(p)} \cdot \frac{1}{M} \right| \leq |n| \right), \quad (3)$$

$$n \in \mathbb{R}, \quad M \in [f_{min}, f_{max}]$$

where $N_r(p)$ denotes the number of equidistant pixels for the pixel p . Coefficient M is defined as $M = |f(p) - f_{desired}|$, where $f_{desired}$ indicates the average value of the scope of gray scale values of the object we want to segment. The closer the value of the point $f(p)$ is to the desired value $f_{desired}$, the closer the newly assigned value $d_n(p)$ is to zero. We will show later that for the values of M approaching zero for a certain object, we will be able to segment the object for a wider range of segmentation coefficient n . If there is no preferred value of the objects to be segmented, a constant value of the coefficient M can be used $M = const$, which assigns the same weighting factor to all gray scale values. In this case, the newly calculated value of the point $d_n(p)$ does not depend on the original point value $f(p)$, but only on the values of equidistant points of the point p . The results for the proposed method are illustrated in Fig. 1. We observe that

with the increase of segmentation coefficient n , only circle-like structures with values close to $f_{desired}$ are preserved.

A. Segmentation by comparison to maximum distance

For each of the transformed images in Fig. 1 a certain pattern in the background of the objects of interest can be observed. We propose an approach for segmentation that separates foreground objects from this background pattern. As shown in (4), for each value M there exists a coefficient value n_{min} , for which the radius growing condition is always fulfilled:

$$n_{min} = \left\lfloor f_{max} \cdot \frac{1}{M} \right\rfloor \quad (4)$$

For example, if $M = f_{max} = const$ and $n = n_{min} = 1$ each pixel p will be assigned a new value $d_n(p)$ equal to the maximum Euclidean distance d_{max} from the pixel p to any other pixel in the image (5),

$$d_{max}(p) = \max_{\forall (x,y) \in I} \left(\sqrt{(x-x_p)^2 + (y-y_p)^2} \right) \quad (5)$$

as represented in Fig. 1f. A straightforward way to segment the objects in the image is to separate the background pixels (pixels with value $d_{max}(p)$) from the foreground pixels (pixels with value different than $d_{max}(p)$), (6),

$$L_n(p) = \begin{cases} 1, & d_n(p) \neq d_{max}(p) \\ 0, & d_n(p) = d_{max}(p) \end{cases} \quad (6)$$

where $L_n(p)$ denotes the decision making function. Results for this segmentation algorithm are presented in the second row of Fig. 2. An important observation is that the maximum possible value that can be assigned to each pixel depends on the size of the image, but this does not affect the segmentation result. This means that the proposed segmentation algorithm depends only on the coefficient n . The drawback of the proposed method is that the distance calculation is computationally demanding, which can make it inefficient for use on larger images. We propose a solution to this problem by using a threshold value for segmentation.

B. Segmentation by thresholding

In order to enhance the computational efficiency of the proposed method, we introduce a threshold in the calculation of the new value for the pixel as shown in (7):

$$d_{n,t}(p) = \max_R (\forall r \in \{1, \dots, R\}, r \leq t, |a| \leq |n|), \quad (7)$$

$$a = \frac{S_r(p)}{N_r(p)} \cdot \frac{1}{M}, \quad n \in \mathbb{R}, \quad t \in \mathbb{N}, \quad M \in [f_{min}, f_{max}]$$

The decision making function in this case is defined in (8).

$$L_{n,t}(p) = \begin{cases} 1, & d_n(p) < t \\ 0, & d_n(p) \geq t \end{cases} \quad (8)$$

This method incorporates the segmentation process directly into the calculation of new pixel values. The calculation holds when the predefined threshold value is reached and in that way needless computations are not performed. The introduction of a threshold raises a question of choosing the threshold value. The pixel with the largest newly assigned

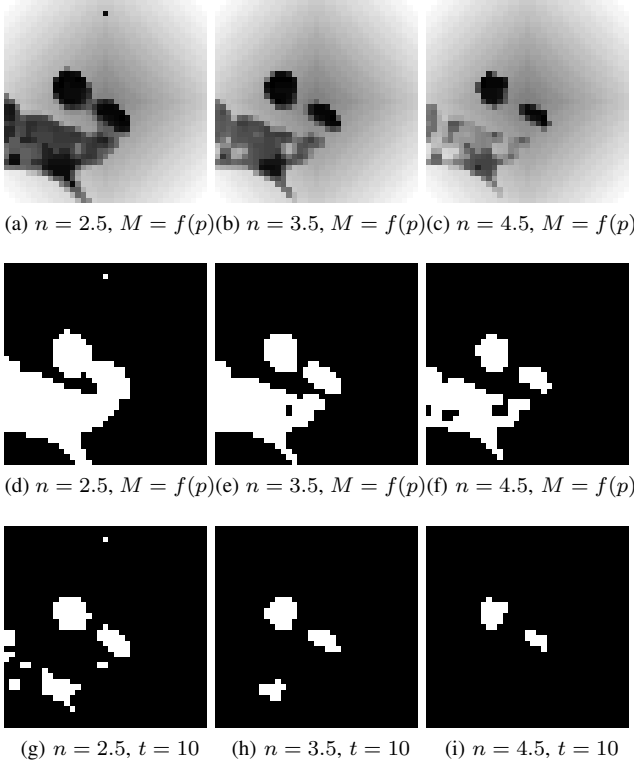


Fig. 2: Transformed images for different values of parameter n in (a), (b), (c), corresponding segmentation based on comparison to maximum distance image in (d), (e), (f) and corresponding segmentation based on thresholding in (d), (e), (f). For the optimal threshold value, better segmentation results are obtained for smaller values of n .

value which we want to segment is situated in the center of the object for segmentation with the largest radius. Hence, the optimal threshold value has to be somewhat larger than the largest radius of all the regions that need to be segmented. Also, the threshold value t has to be smaller than the smallest maximum distance $d_{max}(p)$ in the image in order to avoid segmentation of any background pixels. This distance corresponds to the maximum distance of the central pixel in the image and is equal to the radius of the circumscribed circle of the image. According to this, for an image $I_{m \times n}$ containing an object for segmentation of the maximum radius r_{max} , the threshold t has to fulfill the condition stated in (9).

$$r_{max} < t < \frac{\sqrt{m^2 + n^2}}{2} \quad (9)$$

Apart from reducing the computational complexity, we can obtain better segmentation results for lower values of segmentation coefficient n if the optimal threshold value is found, as shown in the third row of Fig. 2. The optimal threshold value is not always easy to determine, especially in the case of blood vessels in 3-D images, where the same blood vessel can have great variation in size in different slices. Setting the threshold value equal to the maximum radius value of the blood vessels in the 3-D image resolves

this problem.

C. Algorithm for the 3-D segmentation

The 3-D segmentation algorithm can be realized by extending a 2-D version of the proposed method. However, the 3-D version of the proposed method would be computationally demanding for large data sets, which would significantly prolong the execution time. On the other hand, if the seed points for region growing for each slice of the 3-D image are well selected, the 2-D version can be efficiently applied for the segmentation of the whole 3-D set. We propose a region growing algorithm that builds on the previously described method for segmentation criteria. In the first slice the initial seed point has to be selected, after which the region growing is performed and new seed points are calculated for the next slice based on the previously segmented area. This principle is repeated iteratively for each slice in the 3-D image. Each value of the segmentation coefficient n produces one segmented candidate image. After a sufficient number of segmented candidates have been generated, we choose the one that is the most similar to the previous segmented slice by comparing segmented areas, inner radii of regions, center point distances and overlapping areas of segmented regions. Different candidates can also be obtained by varying the threshold parameter t . This approach causes many recalculations without showing significant difference in segmented candidate images. Instead, we propose to keep the threshold at a predefined constant level, and to vary only parameter n . Our idea is to find the maximum ratio of the average value of the equidistant neighborhood and the value of the processed pixel for the threshold $t \in \mathbb{N}$ number of radii, as shown in (10).

$$d_t(p) = \max_{r \in \{1, \dots, t\}} \left(\left| \frac{S_r(p)}{N_r(p)} \cdot \frac{1}{M} \right| \right). \quad (10)$$

Knowing the value $d_t(p)$, the pixel can be segmented for different values of n only by comparing these two values, as in (11).

$$L_{n,t}(p) = \begin{cases} 1, & d_t(p) > n \\ 0, & d_t(p) \leq n \end{cases} \quad (11)$$

The significant advantage of this approach is that once the maximum average value for a pixel $d_t(p)$ is calculated, it does not need to be recalculated again for a different segmentation coefficient value n .

D. Skeletonization and length measurement

In order to calculate the length of blood vessels, we use our 3-D skeletonization and graph construction algorithm described in [5] on the segmented 3-D images. Since the spatial resolution of processed data sets is poor, discontinuities in blood vessels in neighboring slices may occur. We apply interpolation to solve this problem as proposed in [6] in the case of segmentation of liver blood vessels, after which we generate the skeleton image and the graph for the segmented 3-D image. The length is calculated by graph convergence and best path selection between user defined starting and ending points in the segmented 3-D image.

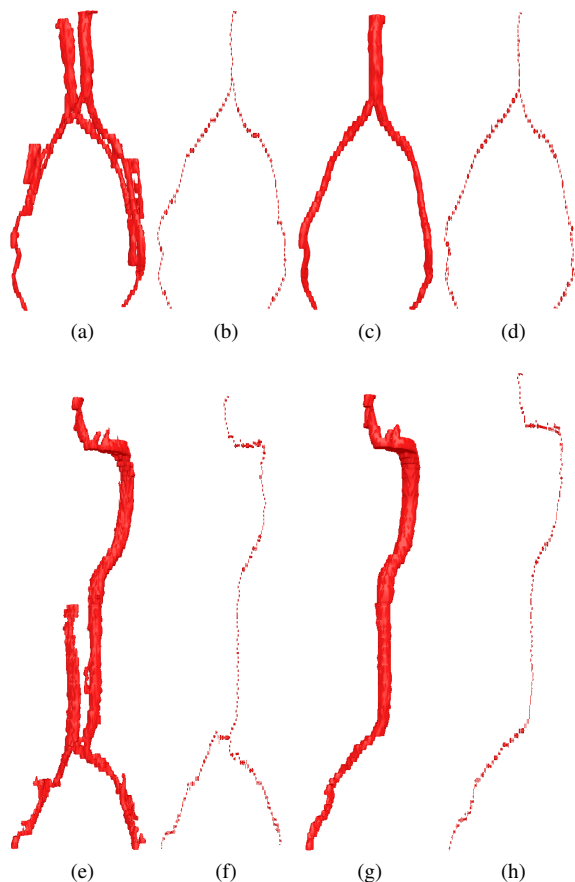


Fig. 3: Segmentation results obtained using the proposed method in (a), (e), and corresponding calculated paths of aortic blood vessels in (b), (f), hand made segmentation in (c), (g) and corresponding calculated paths in (d), (h).

III. RESULTS

We tested our algorithm on five data sets of MRI images of the abdomen, with spacing between slices of 5.5mm and pixel spacing $1.32\text{mm} \times 1.32\text{mm}$. Misalignment, disappearing and merging of blood vessels in neighboring slices is present due to the low resolution. The blood vessels in our data sets were the darkest objects in the image, so we used $f_{desired} = 0$ in our experiments, although this is not the optimal value (the optimal value would be somewhat larger than 0). The segmentation parameter n varied from 2.5 to 4.5 and the threshold value t was set to 30 pixels. In order to evaluate our method, we manually segmented aortic blood vessels in the data sets and measured the lengths by using the same skeletonization and graph construction technique as in our algorithm. Results illustrated in Fig. 3 show that leaks are present in the segmentation, but that they do not affect the skeletonization and path selection. Furthermore, results of length measurements presented in Table I show little deviation between calculated lengths using our algorithm and calculated lengths in manually segmented images. Average execution time of a data set with 100 slices is 15 to 20 minutes on a 2GHz processor.

TABLE I: Calculated lengths for the hand-made segmentation and our segmentation algorithm

Set	Original length (mm)	Our method (mm)	Deviation (%)
1	338	348	2.87
2	337	332	1.48
3	754	722	4.24
4	375	382	1.83
5	381	386	1.29

For the visualization of this dataset we used the *Medical Imaging Interaction Toolkit* (MITK) [7].

IV. CONCLUSION

We introduced a novel method for the segmentation of 2-D and 3-D images with an application to blood vessel length measurements in 3-D abdominal MRI images. We have proposed segmentation approaches based on comparisons to maximum pixel distances and on thresholding. The segmentation based on comparison to maximum pixel distance proved to be easy to set because it uses only parameters n and $f_{desired}$, but is also computationally inefficient. For this reason we introduced a threshold value into the proposed method, which significantly decreased computation time and allowed us to use this method in segmentation of the 3-D data sets. Our automatic method for segmentation of 3-D images stands out in situations when contrast-enhanced images can not be obtained or if the segmentation and length measurement results need to be obtained in a short period of time. An effective algorithm for skeletonization, graph construction and shortest path estimation were used to measure the length of blood vessels of interest. Obtained segmentation results show good resemblance to hand-made segmentation and calculated lengths do not show significant variation compared to calculated lengths of hand-made segmentation. The proposed algorithm can be implemented for segmentation of other organs or tissues in 3-D medical images by varying the segmentation parameters and introducing different conditions for connectivity of regions in neighboring slices.

REFERENCES

- [1] J. Serra: *Image Analysis and Mathematical Morphology*, volume 1, Academic Press, 1982.
- [2] M. Pesaresi, J. A. Benediktsson: *A New Approach for the Morphological Segmentation of High-Resolution Satellite Imagery*, IEEE Trans. Geosci. Remote Sens., vol.39, no. 2, Feb. 2001.
- [3] Bellens, R.; Gautama, S.; Martinez-Fonte, L.; Philips, W.: *Improved classification of urban areas with pixel-based measures of object size*, Proceedings of 28th EARSeL Symposium, Istanbul, Turkey, (2008).
- [4] Kovács T., Cattin P., Alkadhi H., Wildermuth S., Székely G.: *Automatic Segmentation of the Vessel Lumen from 3D CTA Images of aortic Dissection*, Bildverarbeitung für die Medizin 2006: 161-165.
- [5] Babin, Danilo; De Bock, Johan; Pižurica, Aleksandra; Philips, Wilfried: *The shortest path calculation between points of interest in 3-D MRI images of blood vessels*, ProRISC Proceedings (2008): 295-298.
- [6] C. Park, E. Cho, Y. Kwon, M. Park, J. Park: *Automatic Separate Algorithm of Vein and Artery for Auto-segmentation Liver-Vessel from Abdominal MDCT Image Using Morphological Filtering*, Lecture notes in computer science, Springer (2005): 1069-1078.
- [7] *The Medical Imaging Interaction Toolkit*, <http://www.mitk.org>